2014 International Symposium on Nonlinear Theory and its Applications
NOLTA2014, Luzern, Switzerland, September 14-18, 2014

Two-dimensional optical bistable device with external feedback for pulse propagation and spatio-temporal instability

Takashi ISOSHIMA and Yoshihiro ITO

Nano Medical Engineering Laboratory, RIKEN
2-1 Hirosawa, Wako, Saitama 351-0198, Japan
Email: isoshima@riken.jp

Abstract– A bistable device with a spatial expanse can present traveling wavefront at which regions in different stable states (ex. "on" and "off" states) are adjacent to each other. We have reported that a two-dimensional optical bistable device (2DOBD) is one of such devices, and the wavefront propagation can be controlled by the irradiated light intensity. Utilizing expansion and reduction modes of the wavefront propagation, maze exploration was demonstrated by numerical simulation.

In this paper, we introduce external feedback to 2DOBD to realize more complexed spatio-temporal behavior. Refractory feedback, which mimics refractory period of a neuron provides excitability, generates propagating pulses rather than traveling wavefront. Delayed feedback provides spatio-temporal instability, resulting into oscillatory and chaos-like behavior along with spontaneous spatial inhomogeneity. Such a complex spatio-temporal behavior is expected to contribute realization of natural computation.

1. Introduction

In a spatially expanded bistable device, the two stable states (here we assign the terms "on" and "off" to these states) can coexist occupying adjacent area and their boundary can migrate, i.e. a kind of wavefront propagation can occur [1]. Similarly, a spatially expanded excitable system can show pulse propagation, as in a Belouzov-Zhabotinskii (BZ) reaction system or a neural network system. We have been interested in such wavefront or pulse propagation in terms of natural (physical) computation to achieve novel information processing scheme, and investigated various two-dimensional optical bistable devices to realize a variety of functions including maze exploration [2]. Logic operation of AND, OR, and NOT were also demonstrated so that 2DOBD is logically universal.

To demonstrate this experimentally, we propose a simple opto-thermal device structure shown in Fig.1. This device is composed of a temperature-dependent optical transmission layer (top layer) and a black light-absorbing layer (bottom layer). The bottom black layer absorbs light transmitted through the top layer, converting light to heat. Temperature-dependent optical transmission change in the top layer is realized by phase transition. Materials are selected by the phase transition temperature T_{PT} to be slightly higher than the room temperature: an organic material eicosane melts at about 37 °C, and a liquid crystal 4-Cyano-4'-pentylbiphenyl (5CB) showing nematic-isotropic phase transition at about 35 °C. At a temperature lower than T_{PT}, optical transmission is low due to scattering. At a higher temperature than T_{PT} the material is more transparent. When the device is irradiated with a weak light, transmitted fraction is absorbed by the bottom black layer and the temperature of the device increases slightly. Increase of the light intensity causes increase of the temperature, and at the phase transition temperature a positive feedback starts: increase of transmission by phase transition results in increase of heat generation and temperature, which causes further increase of transmission. Finally the device transit to the high transmission (on) state (turn-on transition). When the light intensity is reduced, transition to the low transmission (off) state occurs at lower light intensity than in the turn-on transition, showing a hysteresis character.

If such a bistable device has a spatial expanse, on-state area and off-state area can coexist occupying adjacent area, and the border (wavefront) can propagate [1]. Assume that the whole device is irradiated with bias light at an intensity of bistability, and that the whole device is initially in the off-state. If one area of the device is irradiated with sufficiently strong light, it locally turns on, and thermal diffusion causes turn-on of the adjacent area, resulting into turn-on wavefront propagation. This can be

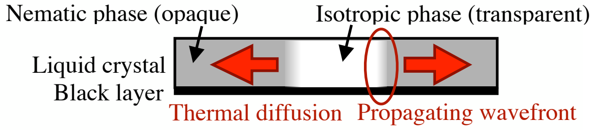

Figure 1: Schematic cross-sectional diagram of an opto-thermal bistable device based on nematic-isotropic phase transition of a liquid crystal. The light irradiated from top transmits through the liquid crystal layer and is absorbed in the black layer to be converted to heat. The liquid crystal presents lower optical transmission due to optical scattering at low temperature in nematic phase, while it shows higher transmission at higher temperature in isotropic phase.

applied to, for example, maze exploration by natural computation [2].

Introduction of external feedback to a nonlinear system can provide diverse and complex dynamics. For example, delayed feedback can generate chaos. Such complex spatio-temporal behavior under external feedback can be a powerful tool for realization of natural computation.

In this paper, we describe numerical simulation of spatio-temporal behavior of our spatially-expanded opto-thermal bistable devices, in order to examine experimental feasibility of the devices. In addition, introduction of external feedback is investigated to achieve more complex behavior: refractory feedback for excitability and pulse propagation, and delayed feedback for chaos-like instability, are examined by numerical simulation.

2. Numerical Simulation Method

The spatially expanded opto-thermal bistable device described above can be formulated with a thermal diffusion equation as follows:

$$\frac{\partial T}{\partial t} = \Delta T + \sigma - \rho \qquad (1)$$

$$\sigma = A(T)\, I \qquad (2)$$

$$\rho = \alpha\, T \qquad (3)$$

where t is the time, T the temperature, σ the generated heat, ρ the heat lost to outside of the device, A the temperature-dependent optical absorption, I the incident light intensity, and α the heat dissipation coefficient (heat resistance).

Numerical simulation was performed by the finite element method using FreeFEM++ software [3]. To simplify the simulation, two-dimensional (2-D) cross section as shown in Fig.1 was used, thus one-dimensional (1-D) wavefront propagation was treated in this paper. To simulate feasible devices, a substrate and a top cover were added at the bottom and top, respectively, of the core structure shown in Fig.1. Glass or acrylic polymer was assumed as the material of the substrate and the top cover. The substrate contacted to a hot plate at 30 or 33 °C (for acrylic polymer cell and glass cell, respectively), and the top cover and side wall of the device were exposed to air at 25 °C. Thicknesses of the top cover, 5CB or eicosane layer, black layer, and substrate were 0.2, 0.1, 0.02, and 1.0 mm, respectively. Optical absorption of the black layer was 100 %. Thermal diffusion constant of glass, acrylic polymer, 5CB, and eicosane were 6.7, 0.92, 1.0, and 2.0 [10^{-3} cm^2 s^{-1}], respectively. Heat dissipation constant (heat resistance) at the boundary of the devices was 0.92×10^{-2} [W $°C^{-1}$]. Division number in vertical direction was 140, and in lateral direction, division number was selected so that the element size became 0.04-0.08 mm. Time step was 0.1 sec. Temperature-dependent transmission of 5CB and eicosane layer was assumed to be 0.5 at lower than 35 °C, 1.0 at higher than 37 °C, and linearly increasing from 0.5 to 1.0 in the temperature range of 35 to 37 °C. Bias light intensity was in the range between 0.25 and 0.5 W/cm^2 depending on the materials and configurations, and it was reduced when feedback was applied. Trigger light intensity was 1.0-2.0 W/cm^2.

3. Results and Discussions

3.1. Wavefront Propagation

Propagation of the wavefront between on- and off-state area was investigated. Glass and acrylic polymer as the cell (substrate and top cover) were compared in 4 mm length devices. In Fig.2, spatial profiles of temperature-dependent transmission at interval of 1 sec are superimposed. The trigger light was irradiated at the center of the devices (at 1.8-2.2 mm position) for 1 sec. In the glass cell device, wavefront width was in the range of 0.8-1.0 mm, and wavefront velocity was in the range of 0.10-0.13 mm/sec. On the other hand, the acrylic polymer cell device presented wavefront width and velocity in the ranges of 0.22-0.38 mm and 0.04-0.10 mm/sec. Here the wavefront width is 10 % - 90 % width, that is the distance between the points where the transmission is 0.55 and 0.95. The wavefront velocity is the velocity of the point where the transmission is 0.75.

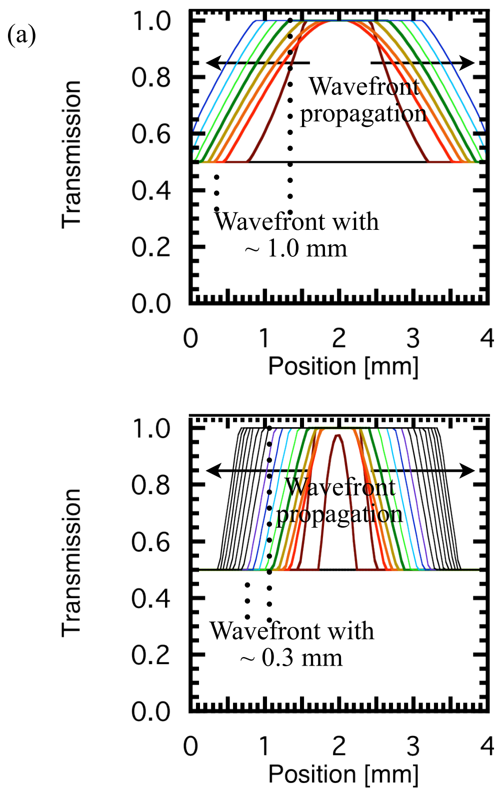

Figure 2: Turn-on wavefront propagation in opto-thermal bistable devices, shown as spatial profiles of optical transmission in eicosane layer, superimposed by 1 sec interval. (a) Eicosane in glass cell. (b) Eicosane in acrylic polymer cell. Device length was 4 mm, bias light intensity of 0.25 W/cm^2. The first (innermost) profile was 2 sec later than the trigger (irradiated at the center = 2 mm position).

The wavefront width of the acrylic polymer cell device is significantly smaller than the glass cell device due to lower thermal conductance (diffusion constant) of the acrylic polymer. Smaller wavefront width is favorable for experiment to realize smaller spatial pattern, thus e.g. more complex maze with the same device size. The wavefront velocity was lower at the edge of the devices, because heat dissipation is larger at the edge. In a device with infinite length, the velocity should be constant in this 1-D propagation.

From experimental point of view, both the wavefront width and velocity are suitable for observation with an ordinary video camera. For complex pattern formation, device length of 4 mm is relatively small, and larger size (e.g. 10 mm or more) is preferable.

3.2. Refractory Feedback

Introduction of external feedback to a nonlinear system can provide diverse and complex dynamics. For example, delayed feedback can generate chaos. Here we investigate effect of external feedback introduced to spatially expanded bistable system. In our devices, we assumed that the transmitted light through the device was (experimentally) observed with a video camera to achieve external feedback. Although optical absorption of the black layer was 100 % in our numerical simulation, we can realize a very small optical transmission in experiment. In numerical simulation, we can use the light intensity at the top of the black layer (transmitted through the eicosane layer).

The first external feedback scheme we investigated was refractory feedback. In the refractory feedback, once the observed light intensity becomes larger than a threshold, the bias light at the point is reduced to 45 % of the original intensity for a fixed period (5 sec), resulting into turn-off of the device at the point and making a pulse. Since this behavior is similar to the refractory period in a neural cell, we call it “refractory” feedback.

Figure 3 shows temporal evolution of the optical transmission profile with 4 sec interval. The leftmost (earliest) profile was 8 sec after beginning of the trigger light pulse, which irradiated at the position of the vertical downward arrow. It can be seen that a pulse propagates from left to right at almost constant shape and velocity.

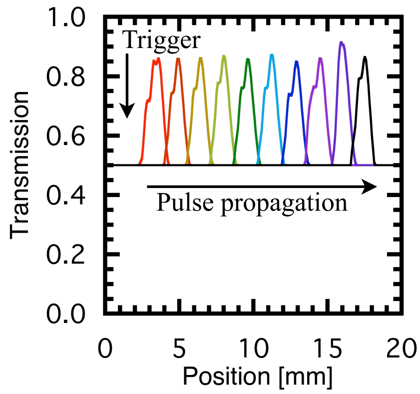

Figure 3: Pulse propagation with refractory feedback, shown as spatial profiles of optical transmission in eicosane layer, superimposed by 4 sec interval. Eicosane in acrylic polymer cell of 20 mm long, bias light intensity of 0.35 W/cm^2. The first (leftmost) profile was 8 sec later than the trigger. Average half-maximum width of the pulses was 1.01 mm, and average pulse velocity was 0.39 mm/sec.

Average pulse width (half-maximum width) was 1.01 mm and average pulse velocity was 0.39 mm/sec. The velocity was higher than the wavefront velocity obtained in section 3.1, possibly because of higher bias light intensity of 0.35 W/cm^2. At lower bias light intensity, the pulse could not sustainably propagate, since reduction of light intensity by the refractory feedback significantly “cools down” the turning-on area.

Interestingly, the pulse was reflected at the right edge of the device (almost at the position of the rightmost profile), although not shown in Fig.3 to avoid complexity.

3.3. Delayed Feedback

The second external feedback scheme investigated was delayed feedback. In the simulation, proportional feedback was employed using parameters as follows: feedback gain of 2, delay time of 0.5 sec, bias light intensity of 0.4 W/cm^2, and target intensity of 0.2 W/cm^2. No trigger light was used. Figure 4 shows cross-sectional temperature distribution of a short (8 mm long) and a long (50 mm long) devices. Under this condition, the devices presented oscillating behavior with a period

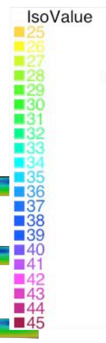

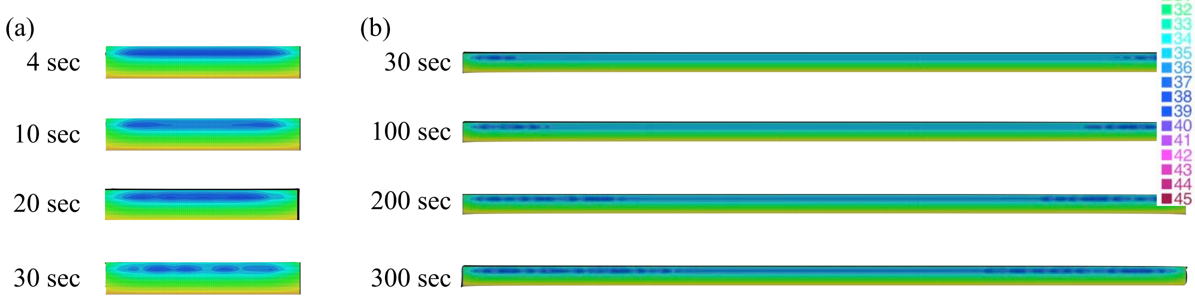

Figure 4: Cross-sectional temperature distribution under delayed feedback. (a) Device with Lateral length of 8 mm, (b) device with lateral length of 50 mm (note that the scaling of the figures is not same as in (a)). Vertical structure is same as described in section 3.1 (length scale of (a) and (b) are different) and both devices are made of eicosane and acrylic polymer. Temperature is shown by color depicted at the right end. Bias light intensity is 0.4 W/cm^2, delay time for feedback is 0.5 sec, and proportional feedback gain is 2.

of *ca.* 1.1 sec, at first uniformly in lateral direction (except for the edges). After some time (~10 sec), spatial nonuniformity emerged, getting more and more nonuniform with time (Fig.4(a)). In the longer device shown in Fig.4(b), it can be seen that nonuniform areas are localized near the edges of the device, and the nonuniform areas expanded toward center with time. These results suggest that the spatial instability (nonuniformity) originates from the edge and it propagates to the center area. It is possible that the spontaneous oscillation frequency is slightly different between the edge and center area due to different heat dissipation condition. Neighboring areas of the device are a kind of coupled (nonlinear) oscillators, and difference in their resonance frequency can cause beat and chaotic behavior. However, whether the nonuniform and unstable behavior is chaos or not is not confirmed yet. Chaos properties such as sensitivity to initial condition (Lyapunov exponent) are now under investigation.

4. Concluding Remarks

In this paper, we have demonstrated by the finite element method calculation that experimentally feasible opto-thermal bistable devices with spatial expanse can present wavefront propagation. It was shown that a device using a lower heat conducting material with a smaller thermal diffusion constant such as acrylic polymer presents smaller wavefront width, i.e. sharper wavefront, compared with a device using a higher heat conducting material such as glass. Wavefront width (0.2-1.0 mm) and velocity (~0.1 mm/sec) are suitable for experimental observation with an ordinary video camera.

We have also examined external feedback so that it can realize more complex dynamics and function to the spatially-expanded opto-thermal bistable devices. It was demonstrated that refractory feedback provides pulse propagation like in a neural cell, in contrast to expansion of on-state area in a device without feedback. With delayed feedback, the device present spontaneous oscillation, at first spatially uniform and later getting nonuniform spontaneously. This spontaneous spatial instability is suggested to originate from the edges of the device. Examination of chaos properties in this behavior is now in progress.

These spontaneous pattern-rhythm formation can be applied to various computational problems such as maze exploration, and our two-dimensional opto-thermal bistable device is an experimentally feasible candidate for natural computation.

Acknowledgments

This work is financially supported by Japan Society for the Promotion of Science (Grant-in-Aid for Scientific Research No.26540129). T. I. acknowledges Dr. Youichi Okabayashi, Dr. Song-Ju Kim, and Dr. Etsushi Nameda for fruitful discussion.

References

[1] J. D. Murray, "*Mathematical Biology I: An Introduction - Third Edition*," Chapter 13, Springer Science+Business Media, New York, 2001.
[2] Y. Okabayashi, T. Isoshima, E. Nameda, S. Kim, M. Hara, “Two-Dimensional Nonlinear Fabry-Perot Interferometer: An Unconventional Computing Substrate for Maze Exploration and Logic Gate Operation.,” *Int. J. Nanotech. Mol. Comp.*, Vol.3, p.13, 2011.
[3] Université Pierre et Marie Curie and Laboratoire Jacques-Louis Lions, *FreeFEM++*, http://www.freefem.org/ff++/